

# Unmanned Aerial Vehicle Guidance for an All-Aspect Approach to a Stationary Target

## **Group - 15**

Abel Viji George AE21B001

Abhigyan Roy AE21B002

Shreeya Padte AE21B056

Indian Institute of Technology  
Madras

November 8, 2024



# Introduction

This study focuses on developing a multiphase guidance algorithm for a UAV in the nonlinear engagement framework that enables an aerial vehicle to approach a stationary target from any direction. The challenges faced by the standard and two-phase Pure Proportional Navigation, mainly approach angle control are addressed, providing solutions that take into account the restrictions imposed by the seeker's field of view (FOV).

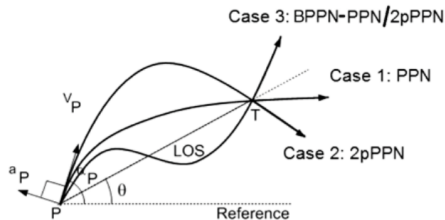


Figure 1: Possible terminal heading of UAV to a stationary target



- ① Importance of controlling approach angles for effective UAV operations.
  - Necessity of controlling terminal path angles includes requirements like efficient way-point navigation, achieving rendezvous, and other desired formations following a trajectory with sensing.
  - Controlling impact angle also becomes important in successful interception against stationary or slowly moving targets, such as aircraft carrier warships with efficient electronics countermeasures and a close-in weapon system.
  
- ② Previous studies and their limitations.



# Previous Studies on Impact Angle-Constrained Guidance Problem

## Linearized Geometry-Based :

Work	Main Focus
1	Optimal-angle-based control guidance.
2	Sliding-mode-control-based guidance.
3	Zero-effort collision triangle was incorporated in a linear optimal guidance problem.

**Limitation :** The optimal-control-based approaches rely on linearization of the engagement problems and are sensitive to the time-to-go estimation error, while the sliding-mode-based approaches have limitations in dealing with scenarios with a relatively large initial heading error causing a positive initial range rate.

<sup>1</sup>Idan, M., Golan, O., and Guelman, M., "Optimal Planar Interception with Terminal Constraints," \*Journal of Guidance, Control, and Dynamics\*, Vol. 18, No. 6, Nov.–Dec. 1995, pp. 1273–1279. doi:10.2514/3.21541

<sup>2</sup>Kumar, S. R., and Ghose, D., "Three-Dimensional Impact Angle Guidance with Coupled Engagement Dynamics," \*Journal of Aerospace Engineering\*, Vol. 231, No. 4, April 2017, pp. 621–641. doi:10.1177/0954410016641442

<sup>3</sup>Cho, H., Ryoo, C. K., Tsourdos, A., and White, B., "Optimal Impact Angle Control Guidance Law Based on Linearization About Collision Triangle," \*Journal of Guidance, Control, and Dynamics\*, Vol. 37, No. 3, May–June 2014, pp. 958–964. doi:10.2514/1.62910



# Previous Studies contd.

## PN-Based :

Work	Main Focus
<sup>4</sup>	Time-varying biased pure PN.
<sup>5</sup> , <sup>6</sup>	Two-stage planar pure PN (2pPPN) for stationary and lower-speed targets.
<sup>7</sup>	Composite PN-based guidance for higher-speed targets.

**Limitation :** They considered the impact-angle control for two-dimensional engagements and did not consider the FOV constraints.

---

<sup>4</sup>Kim, B. S., Lee, J. G., and Han, H. S., "Biased PNG Law for Impact with Angular Constraint," \*IEEE Transactions on Aerospace and Electronic Systems\*, Vol. 34, No. 1, Jan. 1998, pp. 277–288. doi:10.1109/7.640285

<sup>5</sup>Ratnoo, A., and Ghose, D., "Impact Angle Constrained Interception of Stationary Targets," \*Journal of Guidance, Control, and Dynamics\*, Vol. 31, No. 6, Nov.–Dec. 2008, pp. 1817–1822. doi:10.2514/1.37864

<sup>6</sup>Ratnoo, A., and Ghose, D., "Impact Angle Constrained Guidance Against Nonstationary Nonmaneuvering Targets," \*Journal of Guidance, Control, and Dynamics\*, Vol. 33, No. 1, Jan.–Feb. 2010, pp. 269–275. doi:10.2514/1.45026

<sup>7</sup>Ghosh, S., Ghose, D., and Raha, S., "Composite Guidance for Impact Angle Control Against Higher Speed Targets," \*Journal of Guidance, Control, and Dynamics\*, Vol. 39, No. 1, Jan. 2016, pp. 98–117. doi:10.2514/1.G001232



## 2-D Engagement Geometry

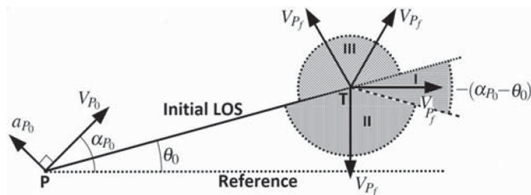


Figure 2: 2-D engagement geometry and UAV's terminal heading.

### Engagement Equations for Stationary Target

$$\dot{R} = V_R = -V_P \cos(\alpha_P - \theta)$$

$$\dot{\theta} = \frac{V_\theta}{R} = -V_P \sin(\alpha_P - \theta)$$

$$\dot{\alpha}_P = \frac{a_P}{V_P}$$

The UAV's look angle is defined as  $\mu = \alpha_P - \theta$

- The UAV's lateral acceleration is based on the pure PN (PPN) guidance law with the navigation gain  $N$  given by,

$$a_P = V_P \dot{\alpha}_P = N V_P \dot{\theta} \quad (1)$$



- The UAV's lateral acceleration is based on the pure PN (PPN) guidance law with the navigation gain  $N$  given by,

$$a_P = V_P \dot{\alpha}_P = N V_P \dot{\theta} \quad (1)$$

- Consider  $\alpha_{P_0} \in [\theta_0, \theta_0 + \pi]$ . In this case, from above equations, it follows that the achievable approach angle using the standard PPN guidance is given by

$$\alpha_{P_f} = \alpha_{P_0} + N(\theta_f - \theta_0)$$

- A collision course with a stationary target assumes  $\alpha_{P_f} = \theta_f$

$$\alpha_{P_f} = \frac{(N\theta_0 - \alpha_{P_0})}{(N - 1)}$$





- The UAV's lateral acceleration is based on the pure PN (PPN) guidance law with the navigation gain  $N$  given by,

$$a_P = V_P \dot{\alpha}_P = N V_P \dot{\theta} \quad (1)$$

- Consider  $\alpha_{P_0} \in [\theta_0, \theta_0 + \pi]$ . In this case, from above equations, it follows that the achievable approach angle using the standard PPN guidance is given by

$$\alpha_{P_f} = \alpha_{P_0} + N(\theta_f - \theta_0)$$

- A collision course with a stationary target assumes  $\alpha_{P_f} = \theta_f$

$$\alpha_{P_f} = \frac{(N\theta_0 - \alpha_{P_0})}{(N - 1)}$$

- For  $N \geq 2$  (which is a condition for the bounded terminal lateral acceleration of the UAV), the achievable approach angle using PPN resides in the interval  $\alpha_{P_f} \in [2\theta_0 - \alpha_{P_0}, \theta_0]$ .



- However,  $[2\theta_0 - \alpha_{P_0}, \theta_0) \subset [-\pi + \theta_0, \theta_0)$  which implies that using the standard PPN, a significant portion of the angular interval in the half-space  $[-\pi + \theta_0, \theta_0)$  cannot be achieved. To expand the achievable approach angle set, a two-stage PPN guidance strategy (2pPPN) was introduced.



- However,  $[2\theta_0 - \alpha_{P_0}, \theta_0) \subset [-\pi + \theta_0, \theta_0)$  which implies that using the standard PPN, a significant portion of the angular interval in the half-space  $[-\pi + \theta_0, \theta_0)$  cannot be achieved. To expand the achievable approach angle set, a two-stage PPN guidance strategy (2pPPN) was introduced.
- For impact angles outside  $[2\theta_0 - \alpha_{P_0}, \theta_0)$ , an orientation guidance for the initial phase of missile flight was proposed. The purpose of orientation guidance is to take the missile from  $(\alpha_{P_0}, \theta_0)$  to  $(\alpha_{P_{ORI_f}} = \theta_0, \theta_{ORI_f} = \theta_0 - \pi/2)$ . Thus, the impact band covers  $\alpha_{P_f} \in [-\pi + \theta_0, \theta_0]$ .
- The gain for this phase is:

$$N_{ORI} = \frac{\theta_0 - \alpha_{P_0}}{\theta_0 - (\theta_0 - \pi/2)} = \frac{2}{\pi} |\alpha_{P_0} - \theta_0|$$



**Theorem 1:** Consider  $\alpha_{P_0} > \theta_0$ . A desired approach angle  $\alpha_{P_f}^d \in [2\theta_0 - \alpha_{P_0}, \theta_0)$  could be attained by PPN with  $N = \frac{\alpha_{P_f}^d - \alpha_P}{\alpha_{P_f}^d - \theta} \geq 2$ , whereas  $\alpha_{P_f}^d \in [-\pi + \theta_0, 2\theta_0 - \alpha_{P_0})$  could be achieved by 2pPPN with

$$N = \begin{cases} \frac{2}{\pi}(\alpha_{P_0} - \theta_0); & \text{if } \frac{\alpha_{P_f}^d - \alpha_P}{\alpha_{P_f}^d - \theta} < 2 \\ \frac{\alpha_{P_f}^d - \alpha_P}{\alpha_{P_f}^d - \theta}; & \text{if } \frac{\alpha_{P_f}^d - \alpha_P}{\alpha_{P_f}^d - \theta} \geq 2 \end{cases}$$

Examples of trajectories using PPN for  $\alpha_{P_f}^d = -\pi/6$  and 2pPPN for  $\alpha_{P_f}^d = -5\pi/6$  are presented, with and without the look-angle constraint.



**Observation 1:** Consider  $\alpha_{P_0} < \theta_0$ . A desired approach angle  $\alpha_{P_f}^d \in (\theta_0, 2\theta_0 - \alpha_{P_0}]$  could be attained by PPN with  $N = \frac{\alpha_{P_f}^d - \alpha_P}{\alpha_{P_f}^d - \theta} \geq 2$ , whereas  $\alpha_{P_f}^d \in (2\theta_0 - \alpha_{P_0}, -\pi + \theta_0]$  could be achieved by 2pPPN with

$$N = \begin{cases} \frac{2}{\pi} |(\alpha_{P_0} - \theta_0)| & \text{if } \frac{\alpha_{P_f}^d - \alpha_P}{\alpha_{P_f}^d - \theta} < 2 \\ \frac{\alpha_{P_f}^d - \alpha_P}{\alpha_{P_f}^d - \theta} & \text{if } \frac{\alpha_{P_f}^d - \alpha_P}{\alpha_{P_f}^d - \theta} \geq 2 \end{cases}$$

**Observation 2:** If  $\alpha_{P_0} = \theta_0$  or  $\alpha_{P_0} = -\pi + \theta_0$ , then before applying Theorem 1 and Observation 1, an engagement geometry  $(\alpha_P, \theta)$  needs to be attained outside the collision course or inverse collision course by using a finite adjustment pulse bias  $B_{adj}$  satisfying

$$\text{sgn}(B_{adj}) = \begin{cases} -\text{sgn}(\alpha_{P_f}^d - \theta_0) & \text{if } \alpha_{P_0} = \theta_0 \\ \text{sgn}(\alpha_{P_f}^d - \theta_0) & \text{if } \alpha_{P_0} = -\pi + \theta_0 \end{cases}$$



# Three-Phase Composite Guidance

- To overcome the limit of angular spectrum for achievable terminal angles, the reversal of the LOS rate is found to be crucial. This can be facilitated by adding a finite bias profile " $Bsgn(\dot{\theta}_0)$ " to the PPN guidance command for a certain time interval (Biased PPN or BPPN).



# Three-Phase Composite Guidance

- To overcome the limit of angular spectrum for achievable terminal angles, the reversal of the LOS rate is found to be crucial. This can be facilitated by adding a finite bias profile " $B\text{sgn}(\dot{\theta}_0)$ " to the PPN guidance command for a certain time interval (Biased PPN or BPPN).
- For PPN,  $\dot{\mu} = (N - 1)\dot{\theta} = -(N - 1)V_P \sin(\mu)/R$ . Hence, depending on the initial value of  $\mu$ , it monotonically increases or decreases to 0, which implies that  $\dot{\theta}$  is sign-preserving.

## Proof:

- $a_P = NV_P\dot{\theta} + B\text{sgn}(\dot{\theta}_0)$
- $\dot{\mu} = -(N - 1)V_P \sin\mu/R + (B/V_P)\text{sgn}(\dot{\theta}_0)$ .
- From eqn of  $\dot{\theta}$ ,  $\dot{\theta}_0$  decreases (increases) if  $\mu_0 > 0$  ( $\mu_0 < 0$ ). Hence,  $\frac{d|\mu|}{dt} < -(N - 1)V_P |\sin\mu|/R$ . So,  $|\mu|$  goes to zero faster than  $R$  and hence, LOS rate changes sign.



# $\alpha$ CIG Law and Algorithm:

Assume that the initial conditions are such that the desired approach angle is not attainable by the PPN or the 2pPPN guidance laws alone. In that case,

- 1 In phase-1, use BPPN guidance,  $a_P^{\alpha CIG} = NV_P \dot{\theta} + B \operatorname{sgn}(\dot{\theta}_0)$  with  $N = 2$  and  $B > 0$  for an interval from  $t = 0$  to  $t = t_2$ .  $t_2$  is the time at which  $\dot{\theta}$  changes sign.  $\theta(t_2) = \theta_2$ ,  $\alpha_P(t_2) = \alpha_{P_2}$ .





# $\alpha$ CIG Law and Algorithm:

Assume that the initial conditions are such that the desired approach angle is not attainable by the PPN or the 2pPPN guidance laws alone. In that case,

- 1 In phase-1, use BPPN guidance,  $a_P^{\alpha CIG} = NV_P \dot{\theta} + B \text{sgn}(\dot{\theta})$  with  $N = 2$  and  $B > 0$  for an interval from  $t = 0$  to  $t = t_2$ .  $t_2$  is the time at which  $\dot{\theta}$  changes sign.  $\theta(t_2) = \theta_2$ ,  $\alpha_P(t_2) = \alpha_{P_2}$ .
- 2 In phase-2, use BPPN guidance again with  $N < 1$  and  $B > 0$  till a time  $t = t_3$ .  $\theta(t_3) = \theta_3$  such that  $\theta_3 \in [\theta_2, \theta_0]$  or  $\theta_3 \in [\theta_0, \theta_2]$  and  $\alpha_{Pf}^d \in [\theta_0, \theta_3 + \pi]$  or  $\alpha_{Pf}^d \in [-\pi + \theta_3, \theta_0]$  for  $\alpha_{P0} > \theta_0$  or  $\alpha_{P0} < \theta_0$ , respectively.



# $\alpha$ CIG Law and Algorithm:

Assume that the initial conditions are such that the desired approach angle is not attainable by the PPN or the 2pPPN guidance laws alone. In that case,

- 1 In phase-1, use BPPN guidance,  $a_P^{\alpha CIG} = NV_P \dot{\theta} + B \text{sgn}(\dot{\theta}_0)$  with  $N = 2$  and  $B > 0$  for an interval from  $t = 0$  to  $t = t_2$ .  $t_2$  is the time at which  $\dot{\theta}$  changes sign.  $\theta(t_2) = \theta_2$ ,  $\alpha_P(t_2) = \alpha_{P_2}$ .
- 2 In phase-2, use BPPN guidance again with  $N < 1$  and  $B > 0$  till a time  $t = t_3$ .  $\theta(t_3) = \theta_3$  such that  $\theta_3 \in [\theta_2, \theta_0]$  or  $\theta_3 \in [\theta_0, \theta_2]$  and  $\alpha_{Pf}^d \in [\theta_0, \theta_3 + \pi]$  or  $\alpha_{Pf}^d \in [-\pi + \theta_3, \theta_0]$  for  $\alpha_{P0} > \theta_0$  or  $\alpha_{P0} < \theta_0$ , respectively.
- 3 In phase-3, use 2pPPN guidance law  $a_{\alpha CIG} = NV_P \dot{\theta}$  with navigation gain  $N$  defined as  $N = \frac{2}{\pi} |\alpha_{P3} - \theta_3|$  as long as  $(\alpha_{Pf}^d - \alpha_P)/(\alpha_{Pf}^d - \theta) < 2$ ; otherwise, set  $N = (\alpha_{Pf}^d - \alpha_P)/(\alpha_{Pf}^d - \theta)$ . This applies if  $\alpha_{Pf}^d$  lies within  $[2\theta_3 - \alpha_{P3}, \pi + \theta_3]$  or  $[-\pi + \theta_3, 2\theta_3 - \alpha_{P3}]$  for initial conditions  $\alpha_{P0} > \theta_0$  or  $\alpha_{P0} < \theta_0$ , respectively.



# $\mu\alpha$ CIG Law and Algorithm:

Similar to  $\alpha$ CIG Law, but here we have the added constraint of the look angle, which adds a few more additional steps. Given  $\alpha_{P_0}$  and  $\alpha_{P_f}^d$ ,

- 1 Use BPPN,  $a_P^{\mu\alpha CIG} = NV_P\dot{\theta} + B\text{sgn}(\dot{\theta}_0)$  with  $N = 2$  and  $B$  finite and positive until time  $t_1$ , at which  $|\mu|$  becomes just less than  $\mu_s$  if  $|\mu_0| = |\alpha_{P_0} - \theta_0| \in [\mu_s, \pi]$ . Let  $\alpha_P(t_1) = \alpha_{P_1}$  and  $\theta(t_1) = \theta_1$ . Else, if  $|\mu_0| \in [0, \mu_s]$ , then  $t_1 = t_0$ ,  $\alpha_P(t_1) = \alpha_{P_1} = \alpha_{P_0}$ , and  $\theta(t_1) = \theta_1 = \theta_0$ .



# $\mu\alpha$ CIG Law and Algorithm:

Similar to  $\alpha$ CIG Law, but here we have the added constraint of the look angle, which adds a few more additional steps. Given  $\alpha_{P_0}$  and  $\alpha_{P_f}^d$ ,

- 1 Use BPPN,  $a_P^{\mu\alpha CIG} = NV_P\dot{\theta} + B\text{sgn}(\dot{\theta}_0)$  with  $N = 2$  and  $B$  finite and positive until time  $t_1$ , at which  $|\mu|$  becomes just less than  $\mu_s$  if  $|\mu_0| = |\alpha_{P_0} - \theta_0| \in [\mu_s, \pi]$ . Let  $\alpha_P(t_1) = \alpha_{P_1}$  and  $\theta(t_1) = \theta_1$ . Else, if  $|\mu_0| \in [0, \mu_s]$ , then  $t_1 = t_0$ ,  $\alpha_P(t_1) = \alpha_{P_1} = \alpha_{P_0}$ , and  $\theta(t_1) = \theta_1 = \theta_0$ .
- 2 In phase-1, use BPPN guidance,  $a_P^{\mu\alpha CIG} = NV_P\dot{\theta} + B\text{sgn}(\dot{\theta}_0)$  with  $N = 2$  and  $B > 0$  for an interval from  $t = 0$  to  $t = t_2$ .  $t_2$  is the time at which  $\dot{\theta}$  changes sign.  $\theta(t_2) = \theta_2$ ,  $\alpha_P(t_2) = \alpha_{P_2}$ .



# $\mu\alpha$ CIG Law and Algorithm:

- 3 In the phase-2, use the look-angle-constrained bias-shaped BPPN guidance  $a_P^{\mu\alpha CIG} = NV_P\dot{\theta} + B\text{sgn}(\theta_1)$  with  $N < 1$  and  $B > 0$  at time  $t \geq t_2$  as long as, for  $\alpha_{P1} > \theta_1$ ,  $\theta < \alpha_{P_f}^d$  and

$$(N-1)V_P(\theta - \theta_2) < \int_{t_2}^t B dt < (N-1)V_P(\theta - \theta_2) + V_P\mu_s;$$

or for  $\alpha_{P1} < \theta_1$ ,  $\theta > \alpha_{P_f}^d$  and

$$(N-1)V_P(\theta_2 - \theta) < \int_{t_2}^t B dt < (N-1)V_P(\theta_2 - \theta) + V_P\mu_s.$$

upto a time  $\hat{t}$ .  $\theta(\hat{t}) = \hat{\theta}$  and  $\alpha_P(\hat{t}) = \hat{\alpha}_P$ .



# $\mu\alpha$ CIG Law and Algorithm:

- 3 In the phase-2, use the look-angle-constrained bias-shaped BPPN guidance  $a_P^{\mu\alpha CIG} = NV_P\dot{\theta} + B\text{sgn}(\theta_1)$  with  $N < 1$  and  $B > 0$  at time  $t \geq t_2$  as long as, for  $\alpha_{P_1} > \theta_1$ ,  $\theta < \alpha_{P_f}^d$  and

$$(N-1)V_P(\theta - \theta_2) < \int_{t_2}^t B dt < (N-1)V_P(\theta - \theta_2) + V_P\mu_s;$$

or for  $\alpha_{P_1} < \theta_1$ ,  $\theta > \alpha_{P_f}^d$  and

$$(N-1)V_P(\theta_2 - \theta) < \int_{t_2}^t B dt < (N-1)V_P(\theta_2 - \theta) + V_P\mu_s.$$

upto a time  $\hat{t}$ .  $\theta(\hat{t}) = \hat{\theta}$  and  $\alpha_P(\hat{t}) = \hat{\alpha}_P$ .

- If  $\alpha_{P_f}^d \in (\hat{\theta}, \hat{\theta} + \pi]$  or  $\alpha_{P_f}^d \in [-\pi + \hat{\theta}, \hat{\theta})$  for  $\alpha_{P_1} > \theta_1$  or  $\alpha_{P_1} < \theta_1$ , respectively, then  $t_3 = \hat{t}$ ,  $\alpha_{P_3} = \hat{\alpha}_P$ , and  $\theta_3 = \hat{\theta}$ . Begin the third phase as specified in Step 4.
- Continue with the look-angle-constrained BPPN guidance  $a_P^{\mu\alpha CIG} = NV_P\dot{\theta} + B\text{sgn}(\theta_1)$  with  $N = 1$  and  $B = 0$  until  $\theta = \theta_3$  at some time  $t_3$  such that  $\alpha_{P_f}^d \in (\theta_3, \theta_3 + \pi]$  or  $\alpha_{P_f}^d \in [-\pi + \theta_3, \theta_3)$ , if  $\hat{\theta} < -\pi + \alpha_{P_f}^d$  or  $\hat{\theta} > \pi + \alpha_{P_f}^d$  for  $\alpha_{P_1} > \theta_1$  or  $\alpha_{P_1} < \theta_1$ , respectively, let  $\alpha_P(t_3) = \alpha_{P_3}$ . At time  $t = t_3$ , start the third phase as in Step 4.



## 4 In phase-3,

- Use PPN guidance with  $a_P^{\mu\alpha CIG} = NV_P \dot{\theta}$ , where  $N = (\alpha_{P_f}^d - \alpha_{P_3})/(\alpha_{P_f}^d - \theta_3)$ , if  $\alpha_{P_f}^d \in (\theta_3, 2\theta_3 - \alpha_{P_3}]$  or  $\alpha_{P_f}^d \in [2\theta_3 - \alpha_{P_3}, \theta_3)$  for  $\alpha_{P_1} > \theta_1$  or  $\alpha_{P_1} < \theta_1$ , respectively.
- Use 2pPPN guidance law  $a_P^{\mu\alpha CIG}$  with navigation gain  $N$  defined as  $N = \frac{2}{\pi} |\alpha_{P_3} - \theta_3|$  as long as  $(\alpha_{P_f}^d - \alpha_P)/(\alpha_{P_f}^d - \theta) < 2$ ; otherwise, set  $N = (\alpha_{P_f}^d - \alpha_P)/(\alpha_{P_f}^d - \theta)$ . This applies if  $\alpha_{P_f}^d$  lies within  $(2\theta_3 - \alpha_{P_3}, \pi + \theta_3]$  or  $[-\pi + \theta_3, 2\theta_3 - \alpha_{P_3})$  for initial conditions  $\alpha_{P_1} > \theta_1$  or  $\alpha_{P_1} < \theta_1$ , respectively.



# Simulation Setup and Results

- All the results presented were simulated in MATLAB.
- The target is stationary and in line with the pursuer initially ( $\theta_0 = 0$ )
- The initial angle of the pursuer ( $\alpha_{P0}$ ) is  $45^\circ$  for 2pPPN and  $135^\circ$  for the Three-phase Composite guidance,  $\alpha$ CIG and  $\mu\alpha$ CIG laws.

$\alpha_{P_f}^d$ , rad	Guidance	First phase			Second phase			
		N	B	$t_2$ , s	N	B	$t_3$ , s	$\theta_3$ , rad
0	$\alpha$ CIG	2	$V_P \alpha_P /5$	27.09	-2	$V_P \alpha_P /10$	37.82	-0.071
0	$\mu\alpha$ CIG	2	$V_P \alpha_P /5$	27.29	-2	$V_P \alpha_P /10$	32.57	-0.213
$\pi/3$	$\alpha$ CIG	2	$V_P \alpha_P /5$	27.09	-2	$V_P \alpha_P /10$	37.82	-0.071
$\pi/3$	$\mu\alpha$ CIG	2	$V_P \alpha_P /5$	27.29	-2	$V_P \alpha_P /10$	32.57	-0.213
$5\pi/6$	$\alpha$ CIG	2	$V_P \alpha_P /5$	27.09	-2	$V_P \alpha_P /10$	37.82	-0.071
$5\pi/6$	$\mu\alpha$ CIG	2	$V_P \alpha_P /5$	27.29	-2	$V_P \alpha_P /10$	32.57	-0.213





# Trajectory Analysis and Look Angle for Two Phase PPN (paper)

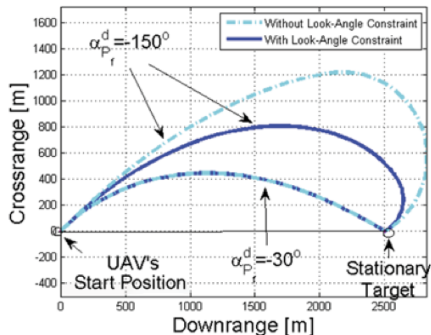


Figure 3: UAV's trajectory for PPN and 2pPPN for  $\alpha_{Pf}^d = -30^\circ$  and  $-150^\circ$ .

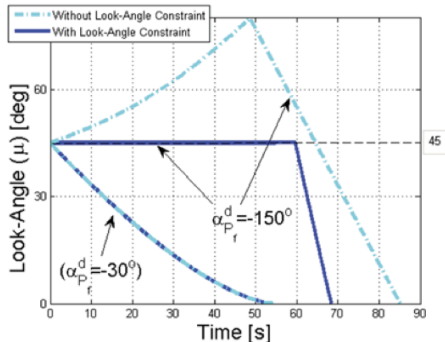


Figure 4: Variation of Look-Angle with time.



# Trajectory Analysis and Look Angle for Two Phase PPN (code)

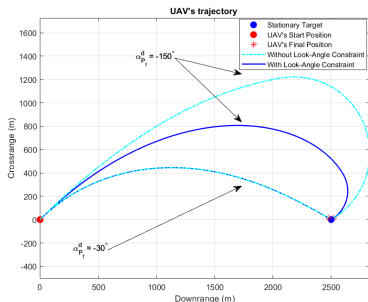


Figure 5: UAV's trajectory for PPN and 2pPPN for  $\alpha_{Pf}^d = -30^\circ$  and  $-150^\circ$ .

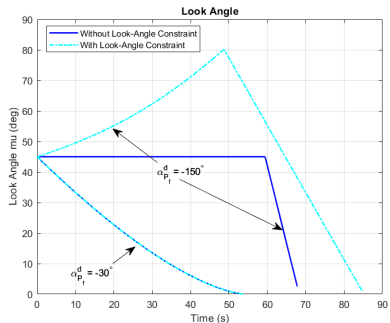


Figure 6: Variation of Look-Angle with time.



# Example of three-phase composite guidance

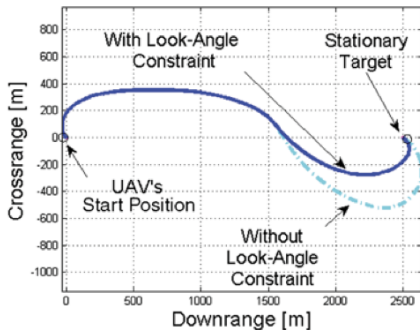


Figure 7: UAV's trajectory for  $\alpha_{pf}^d = 150^\circ$ . (Paper)

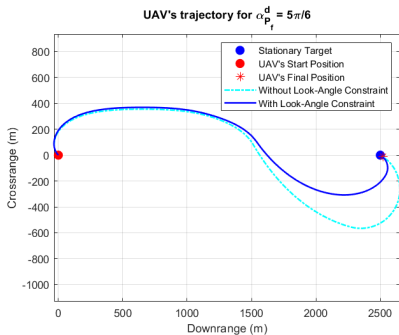


Figure 8: UAV's trajectory for  $\alpha_{pf}^d = 150^\circ$ . (Code)



# 2-D engagement with $\alpha_{P_f}^d = 0$ (paper)

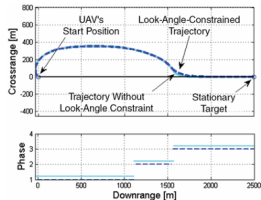


Figure 9: UAV's Trajectory

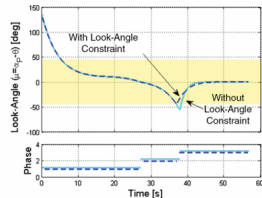


Figure 10: Look-Angle over Time

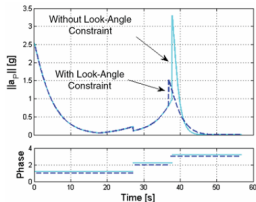


Figure 11: Lateral Acceleration Requirement

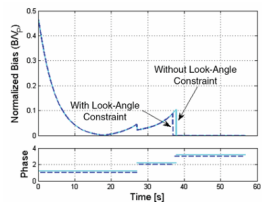


Figure 12: Bias Variation over Time



# 2-D engagement with $\alpha_{P_f}^d = 0$ (code)

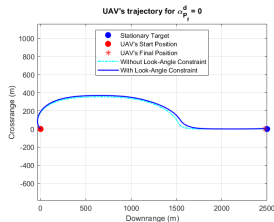


Figure 13: UAV's Trajectory

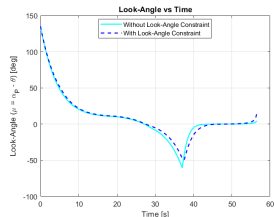


Figure 14: Look-Angle over Time

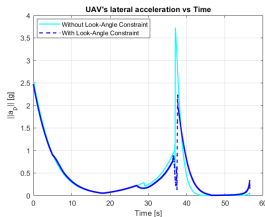


Figure 15: Lateral Acceleration Requirement

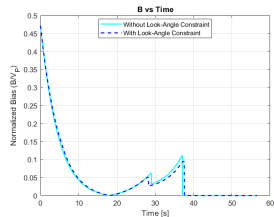


Figure 16: Bias Variation over Time



# 2-D engagement with $\alpha_{P_f}^d = \pi/3$ (paper)

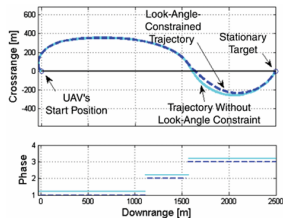


Figure 17: UAV's Trajectory

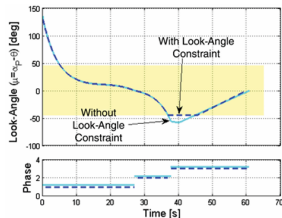


Figure 18: Look-Angle over Time

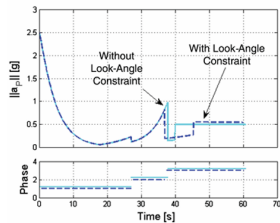


Figure 19: Lateral Acceleration Requirement

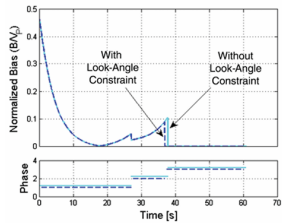


Figure 20: Bias Variation over Time



# 2-D engagement with $\alpha_{P_f}^d = \pi/3$ (code)

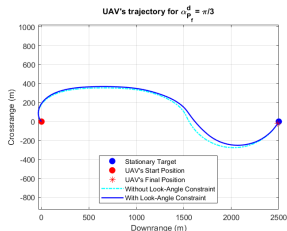


Figure 21: UAV's Trajectory

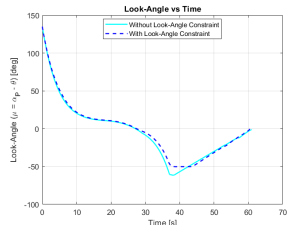


Figure 22: Look-Angle over Time

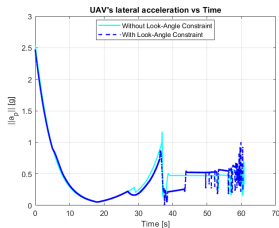


Figure 23: Lateral Acceleration Requirement

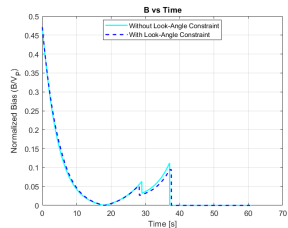


Figure 24: Bias Variation over Time



# 2-D engagement with $\alpha_{P_f}^d = 5\pi/6$ (paper)

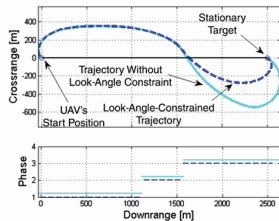


Figure 25: UAV's Trajectory

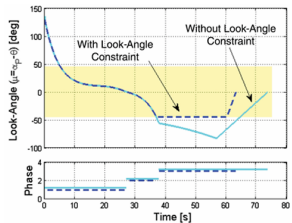


Figure 26: Look-Angle over Time

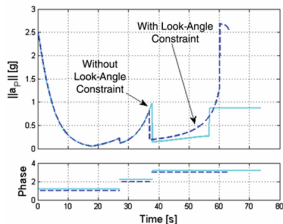


Figure 27: Lateral Acceleration Requirement

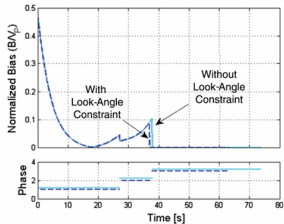


Figure 28: Bias Variation over Time





# 2-D engagement with $\alpha_{P_f}^d = 5\pi/6$ (code)

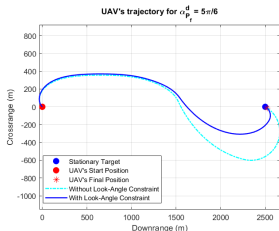


Figure 29: UAV's Trajectory

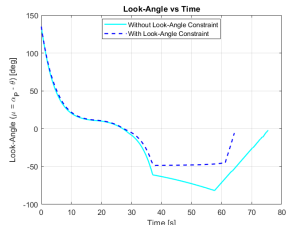


Figure 30: Look-Angle over Time

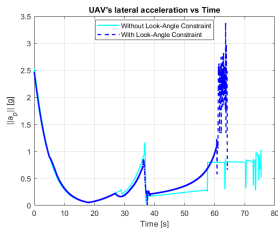


Figure 31: Lateral Acceleration Requirement

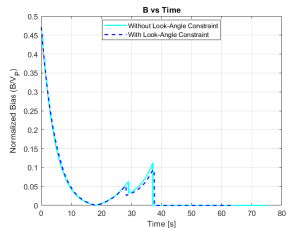
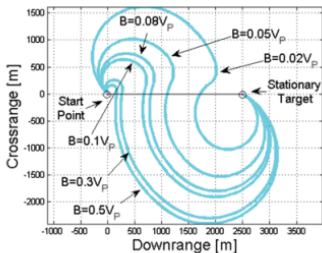


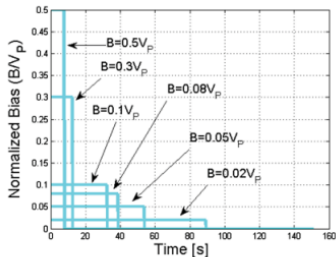
Figure 32: Bias Variation over Time



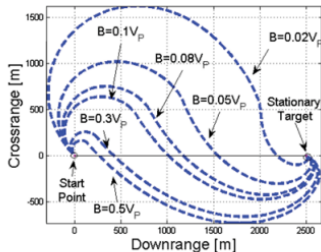
# $\alpha$ CIG and $\mu\alpha$ CIG with varied constant Bias profiles (paper)



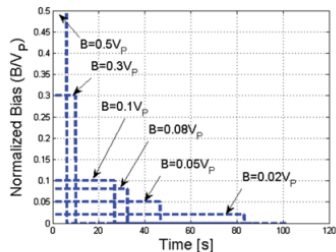
a)  $\alpha$ CIG trajectories



b)  $\alpha$ CIG bias profiles



c)  $\mu\alpha$ CIG trajectories



d)  $\mu\alpha$ CIG bias profiles



# $\alpha$ CIG and $\mu\alpha$ CIG with varied constant Bias profiles (code)

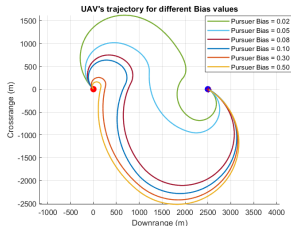


Figure 33:  $\alpha$ CIG Trajectories

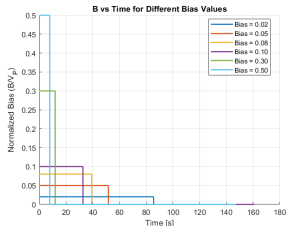


Figure 34:  $\alpha$ CIG Bias Profiles

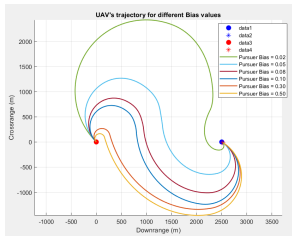


Figure 35:  $\mu\alpha$ CIG Trajectories

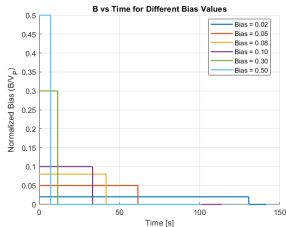


Figure 36:  $\mu\alpha$ CIG Bias Profiles



- As seen, implementing the  $\mu\alpha$ CIG Law , a full circle approach angle set  $[-\pi, \pi)$  can be achieved while satisfying the FOV constraint which gives a bias-shaped BPPN guidance .
- Implications for UAV operations in real-world scenarios and Potential applications of developed guidance strategies.
  - Precision strikes and surveillance missions
  - Infrastructure Inspection
  - Search and Rescue Missions



## Extensions

- Furthering the work in this paper, we can implement a modified law for non-stationary targets, starting with constant velocity targets and extending to maneuvering targets.
- Also, we can add environmental conditions like wind velocity or turbulence like drag as variables in the engagement equations of the UAV.

The paper also has implemented the same for 3D engagements and SITL simulations, which we have not discussed due to time constraints.

